

Noncontact Measurement Techniques for Model Correlation

Peter Avitabile, Chris Niezrecki, Mark Helfrick, Chris Warren, Pawan Pingle,
University of Massachusetts Lowell, Lowell, Massachusetts

There are a variety of different noncontacting measurements that can typically be employed for developing modal test data. Digital image correlation, dynamic photogrammetry, and three dimensional (3D) laser vibrometry are all noncontacting measuring approaches that were used to obtain modal data for a candidate test structure along with traditional accelerometer measurements. Each approach has its benefits and drawbacks, so comparative measurements are made using these devices to show some of the strengths and weaknesses of each technique. Comparisons are made in all cases to a well-studied, finite-element model as well as to each other.

Modal testing can be performed using a variety of different techniques. Accelerometer, laser vibrometer, and stereophotogrammetry measurement systems all have advantages and drawbacks, so each must be implemented where they will be most effectively employed, many times in conjunction with another technique.

Accelerometers are by far the most traditional and widely used sensors employed in modal testing. Their ease of use allows broadband measurements to be made, but one must consider the effects of mass loading, especially at higher frequency ranges. Laser Doppler vibrometers provide a noncontacting, broadband alternative to accelerometers, but large displacements and rigid body motion can contaminate the data dramatically. Conversely, digital image correlation (DIC) and dynamic photogrammetry are both specific applications of stereophotogrammetry that are well suited to measuring large displacements. These displacement-based approaches allow three-dimensional (3D) coordinates of an object (within the field of view) to be tracked by using images (digital or photographic) obtained at two or more known positions in space.

Stereophotogrammetry has been used for many years in the field of solid mechanics to measure full-field displacement and strain, but only very recently has the technique been exploited for dynamic applications to measure vibration.¹⁻⁵ As with laser vibrometry, line of sight with the measurement points must be maintained. Furthermore, surface preparation is generally required for both techniques; a speckle pattern is applied to a test object prior to imaging for DIC, while dynamic photogrammetry tracks high-contrast, circular targets or identifiable features within an image. During postprocessing of the recorded images, image processing is done to correlate similar points in one image to another (tracking gray level variations for the DIC and ellipses for dynamic photogrammetry), thereby identifying dynamic changes to the structure of interest.

To obtain mode shapes from accelerometer and vibrometer FRF measurements, modal parameter estimation must be performed. With both optical-based systems studied in this work, the mode

shapes are measured directly using forced normal mode testing. Dynamic photogrammetry monitors the response at discrete targets, while DIC is capable of providing a relatively continuous measurement – on the order of tens of thousands of points – throughout a continuously patterned surface.

Two structures are considered in this work. The first is a panel structure where only digital image correlation is performed and compared to a finite-element model. The second structure is one used in previous studies and was chosen to compare these four measurement approaches. Test setups and measurement considerations for each case are addressed. Each test is correlated to a well-known and highly accurate finite-element model. Advantages and disadvantages observed are discussed.

About Imaging Techniques

Measurements using lasers and accelerometers have been routinely performed for many years. However, digital image correlation approaches have not been used for structural dynamic measurements and need some discussion. Principles of photogrammetry were first developed as a means to create maps from aerial photographs.⁶ The distances measured on film have a direct relationship to actual distances. The advent of the digital camera and computers replaced film, allowing photogrammetric analysis to be done by a computer. A computer is able to recognize and track a specific point on a series of images through a correlation process. By tracking discrete points in images taken by a stereo pair of cameras and applying photogrammetric principles, shape, strain and displacement can be measured. The geometries involved in a stereo camera setup are described in Figure 1.

The fundamental measurement made is of digitized light intensity values across a rectangular array of pixels embedded in the CCD cameras. Each cell of the array stores a grayscale value typically ranging from 0 to 255, depending on the intensity of the light reflected off the object.

The first pair of images is called the reference image. The computer divides the image into overlapping facets (or subsets), typically 5-20 pixels square. For correlation to work, each facet must carry a unique “fingerprint” of light intensity values. This is why a speckle pattern is applied to the object prior to imaging. A random high-contrast, grayscale pattern works best with speckles having a diameter of about 5-7 pixels when viewed by a camera.⁷ The correlation process is well documented for two-dimensional measurement^{8,9} and for three-dimensional DIC.¹⁰⁻¹²

Prior to testing, the photogrammetric principles of triangulation and bundle adjustment⁶ are used extensively in determining the cameras’ positions relative to each other. DIC packages typically include calibration panels with a series of dots on a rigid flat surface. The calibration panel is sized so that it fills the desired field of view for the measurements to follow. The distance between the dots is input into the software. This allows the position of the cameras relative to each other and the internal distortion parameters of each lens to be accounted for after a series of snapshots of the calibration panel are analyzed by the DIC software. There are other less popular methods and procedures for calibration, but they are not discussed here.

Studies of vibrations often require the measurement of small displacements. Therefore, the sensitivity of DIC measurement must be understood, especially for measurements in the out-of-plane direction. The relation of the pixel size to the object sample size must be known (Figure 2). This is typically done by dividing the width of the field of view by the number of active pixels across

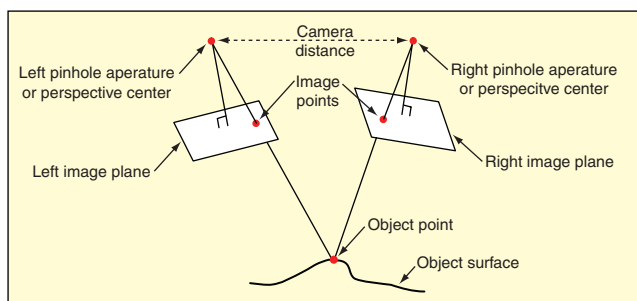


Figure 1. Stereo camera pair allows for two image planes corresponding to one object surface.

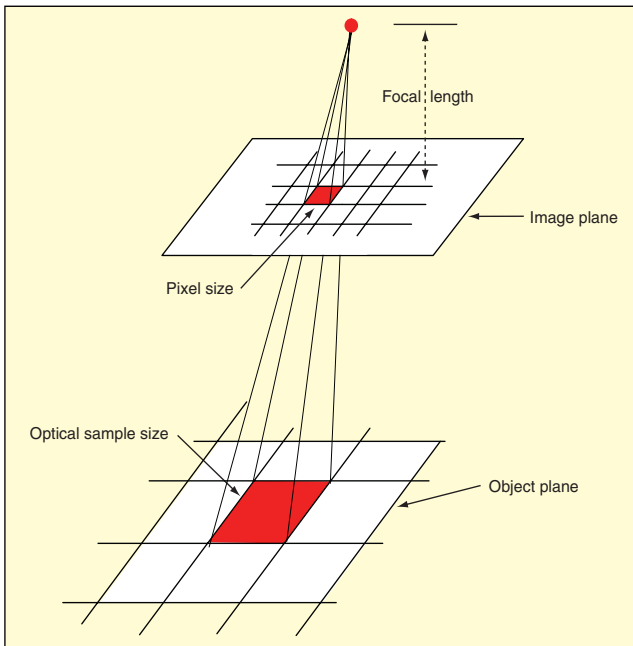


Figure 2. Pixel size in relation to object sample size.

the width of the pixel array to obtain a distance per pixel. The sensitivity will decrease as this number gets larger. For the system tested (Aramis™), the facet pattern matching is iterated until a stability of 0.001 pixels is mathematically reached. The in-plane physical accuracy is approximately 1/100 pixel, while the out-of-plane accuracy is approximately 1/30 pixel.¹³⁻¹⁵ These sensitivity values vary depending on a number of factors, including lighting and speckle pattern effectiveness.

Panel Structure

A formed base panel from a dryer cabinet has been used in previous studies using traditional modal test techniques for correlation to a finite-element model. This panel was used to determine the ability of the digital image correlation technique to obtain suitable data for correlation to the finite-element model. More in depth details of this test and correlation are presented in Reference 2, and only summarized results are presented here to show the capability of the full-field measurement approach.

The metal base of the dryer cabinet was hung in a free-free condition and excited at one corner by a shaker. Two high-speed Photron FastCam APX RS cameras were mounted on a crossbar atop a tripod (Figure 3). The cameras used were capable of capturing images at speeds of up to 10 kHz. For this experiment, images were captured at rates under 3 KHz, which allowed for 15 pictures per cycle. At this frame rate, a 1024 × 1024 array of pixels is the maximum possible. Data were collected for the first three flexible modes of the panel structure using a forced operating mode response approach. The first three operating shapes as captured by DIC are illustrated in Figure 4. The contours of peak z-direction displacement from an initial reference image give a clear indication of how the structure is behaving during each test. The measurement locations that do not have data over the surface (dropouts) are due to the light reflection (camera pixel saturation) and because of the recessed parts of the panel that are not visible to both cameras.

A finite-element model of the dryer cabinet base containing 24,000 nodes had been previously developed for a traditional modal correlation study. This same model was used in the FEM-tools software for correlation with the DIC experimental data. The experimental data points were overlaid on the FEA model by exporting data from the DIC software and converting it to a universal file format. Over 7,500 node points were measured in each of the experimental tests, and more than 24,000 nodes were created in the FEA model (Figure 5). The final correlation allowed for over 7,000 nodes in the experimental results to be paired up with a node from the FEA model. It is extremely important to note the vast number of effective data points that are available from the DIC

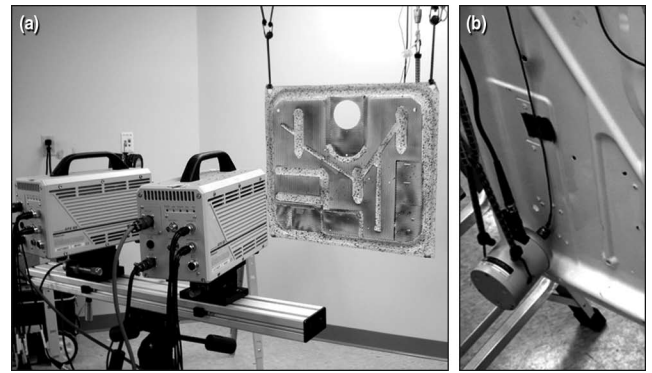


Figure 3. (a) Stereo pair of high-speed cameras aimed at dryer base and (b) mechanical shaker hung from above and connected to the back corner of dryer base.

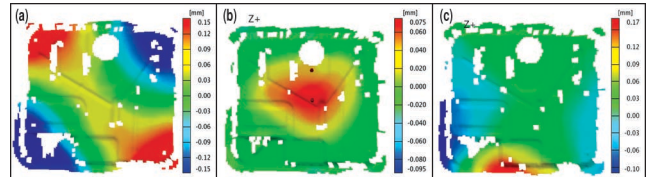


Figure 4. Contours of Z displacement for (a) mode 1; (b) mode 2; (c) mode 3 after filtering.

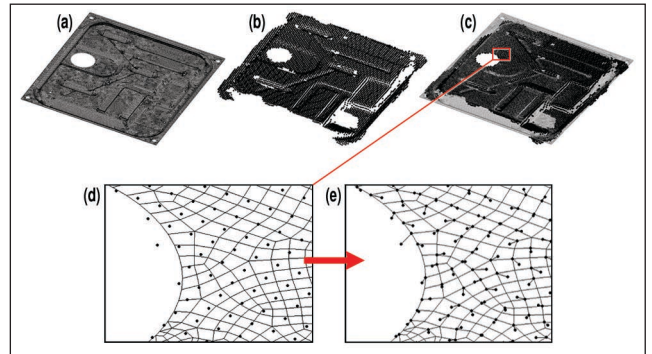


Figure 5. (a) The finite-element model; (b) experimental node positions; (c) experimental node positions overlaid on FEA; (d) close-up of experimental nodes overlaid on the FEA mesh; (e) creation of node pairs.

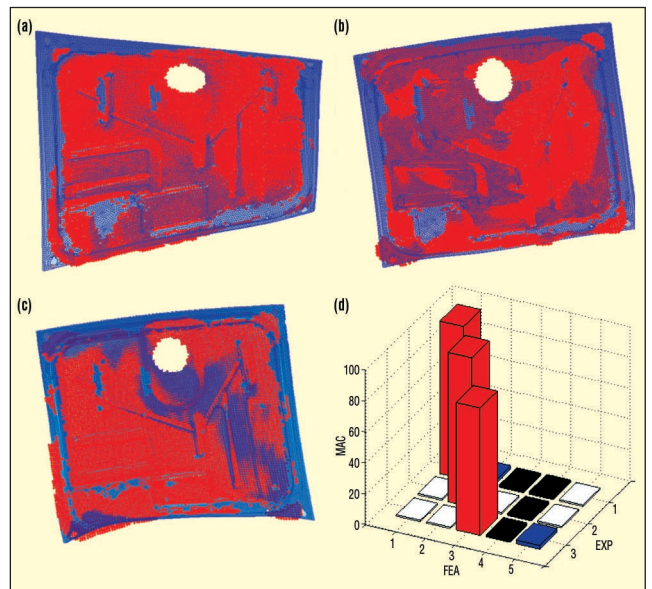


Figure 6. Experimental nodes shown as red dots are overlaid on FEA model for (a) mode 1; (b) mode 2; (c) mode 3; and (d) corresponding MAC values.

test. The three experimental operating shapes were compared to the first five mode shapes of the FEA model (Figure 6). The modal assurance criteria (MAC) provides feedback as to how well the

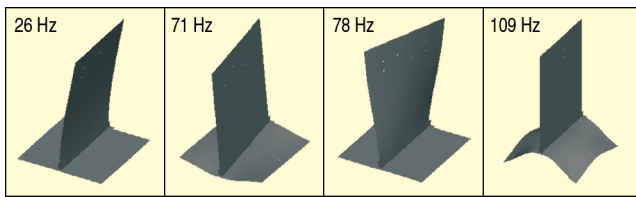


Figure 7. Structural model and its mode shapes for structure under study.

shapes correlated. The first three flexible mode shapes had very good MAC values as seen in the plot in Figure 6d.

Test and Correlation Structure

A generic structure referred to as the BU (base – upright) was used as the test article for all tests presented in this section of the article. The base plate is 24 × 24 inches and rigidly bolted to the floor at four locations, while the upright is 24 × 36 inches. Both plates are 0.75-inch-thick aluminum. A finite-element model is available and has been shown to be very well correlated to other measured test data from previous studies.¹⁶⁻¹⁸ Table 1 summarizes the MAC and pseudo-orthogonality check (POC) results for the accelerometer and laser vibrometer for the first seven modes. In previous work, excellent correlation between both laser and accelerometer measurements and the BU finite-element model was presented.¹⁹ The average frequency difference is less than 2.5%, and the minimum MAC is greater than 0.97 for the first seven modes, confirming that the model is a very good representation of the true structure and therefore a good model to use as a comparison to all of the different measuring approaches studied here. The first four analytical mode shapes of the BU are shown for reference in Figure 7.

Necessary changes in the test setup were made when transitioning from the more traditional modal approaches to DIC and dynamic photogrammetry testing. The two configurations are described in detail below.

Accelerometer and Laser Doppler Vibrometer Test Setup. When the accelerometer and laser data were acquired, shaker excitation was provided at an angle 45° relative to all three principle axes so that all modes would be excited. The excitation was pseudorandom over a 400 Hz bandwidth. Thirty averages were taken with 1600 lines of spectral resolution to obtain adequate coherence over the frequency range of interest. Figure 8a depicts a shaker mounted to the BU with the laser and accelerometer measurement points indicated by red dots and their numbers. Figure 8b displays an overlay of FRFs measured by an accelerometer and the laser Doppler vibrometer at point 3. A frequency domain, polynomial curvefitter available in the LMS Modal software²⁰ was then used to extract the modal parameters and mode shapes.

DIC and Dynamic Photogrammetry Test Setup. Both optically based measurement techniques monitored the response of the BU at the same eight locations as in the accelerometer and laser tests. While DIC can be used over the whole surface,² an alternative approach with patches of patterns was employed. (This was done to illustrate that equivalent data could be extracted without having to pattern the entire structure. Note that the panel structure showed results with the entire surface patterned for measurements.) The surface treatment of the BU needed for the DIC test can be seen in Figure 9a. To create the patches, flat white spray paint coated the areas of interest. A black permanent marker was then used to create the speckle pattern. Circular targets with adhesive backs were subsequently applied over the speckle pattern prior to performing the dynamic photogrammetry test. An example of each can be seen

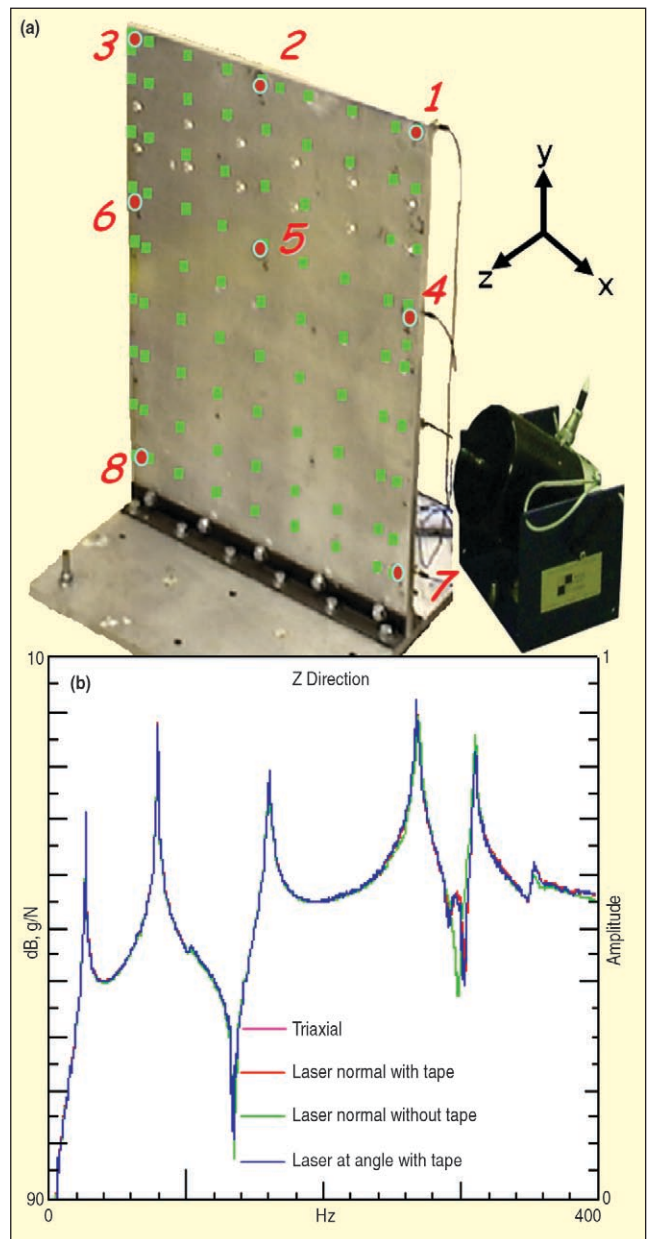


Figure 8. (a) Shaker orientation and measurement points. (b) Sample FRF from previous study [19].

in Figure 10, which shows the entire structure with one patch shown for display of the speckle pattern along with a photogrammetric target. Also shown in the figure is the corresponding set of DIC points and the geometric correlation with the finite-element model. This figure clearly shows the vast amount of data that can possibly be obtained from the DIC system for one patch of data.

Because these systems measure displacements (shapes) directly, forced normal mode testing available in the LMS Modal software²⁰ was conducted to drive the structure at resonance. Two shakers were mounted near the base of the upright, as shown in Figure 9b. The camera pair then captured a series of images throughout two to three cycles using a phase-stepping approach. The amplitude and phase of vibration at eight discrete points were monitored and used as feedback to tune the two shaker inputs so that the BU exhibited single-mode behavior. Figure 9c shows an example of the motion at the same eight points for the 26-Hz mode for one of the dynamic photogrammetry measurements. Note that each signal is in phase, which is to be expected when measuring what is essentially the first bending mode of the upright. The three points along the top of the upright are moving at roughly the same amplitude, while those along the midline move together, etc.

The maximum values of displacement during a test were used when correlating the optical results to the finite-element model,

Table 1. Previous accelerometer and laser Doppler vibrometer results (first seven modes).¹⁹

Correlation Term	Accelerometer Data	Laser Data
Average MAC Diagonal	0.989	0.992
Average MAC Off Diagonal	0.002	0.055
Average POC Diagonal	0.996	0.995
Average POC Off Diagonal	0.021	0.027

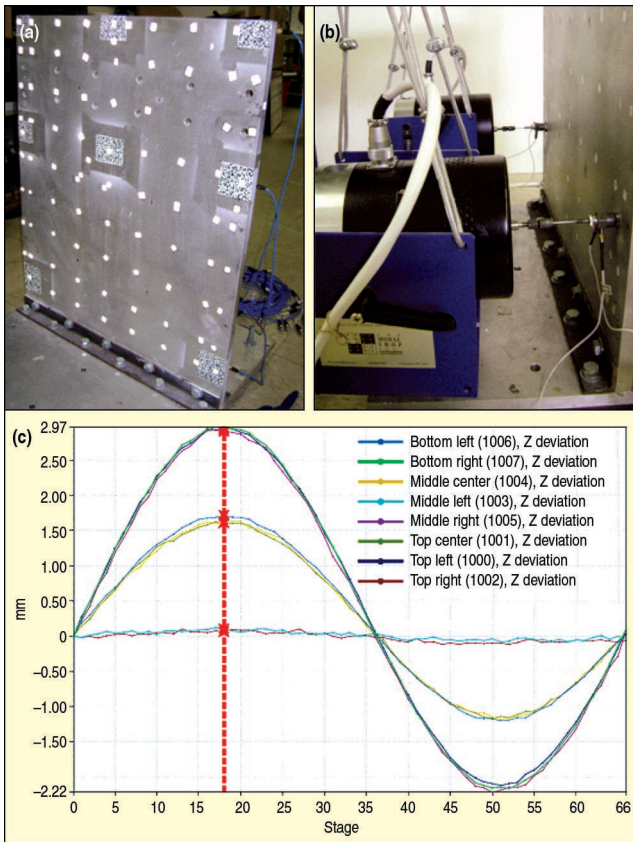


Figure 9. (a) BU patterned at 10 separate locations for DIC testing. (b) Shaker orientation. (c) Sample output from dynamic photogrammetry test.

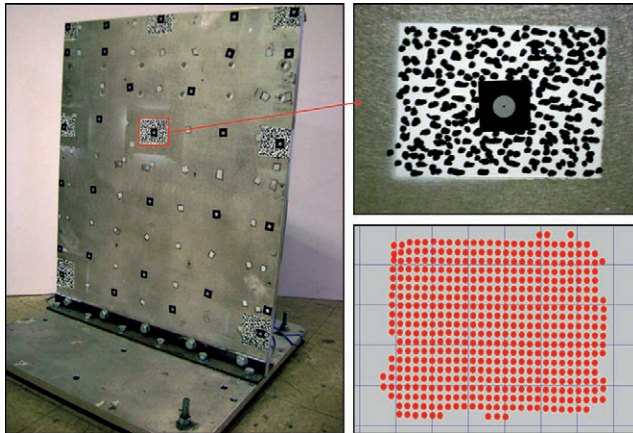


Figure 10. Prepared measurement surface (left) with close-up of one speckle pattern with optical target (upper right) and DIC effective measurement points on top of finite-element mesh of that region (lower right).

laser, and acceleration mode shapes because they naturally have the highest signal-to-noise ratio. In this example, the shape used was measured in Stage 18, indicated by the red cursor in Figure 9a.

When any forced normal mode (FNM) test is run, a variety of shaker configurations are typically needed to excite different mode shapes. For the purposes of the evaluation of this paper, only the bending and torsion modes were considered with the dual shakers set in one configuration; other shaker configurations would be needed to optimally excite other modes of the structure and were not targeted in this study.

One drawback to any displacement-base measurement technique is that relatively high-frequency phenomena cannot be measured due to the low displacements associated with their vibrations. In these tests, which had a working distance of approximately 2 m between the cameras and BU, the out-of-plane noise floor was measured to be approximately 40 μm . For this setup, only the first and third modes of the structure were captured using DIC and dynamic photogrammetry to compare with the other measurement techniques.

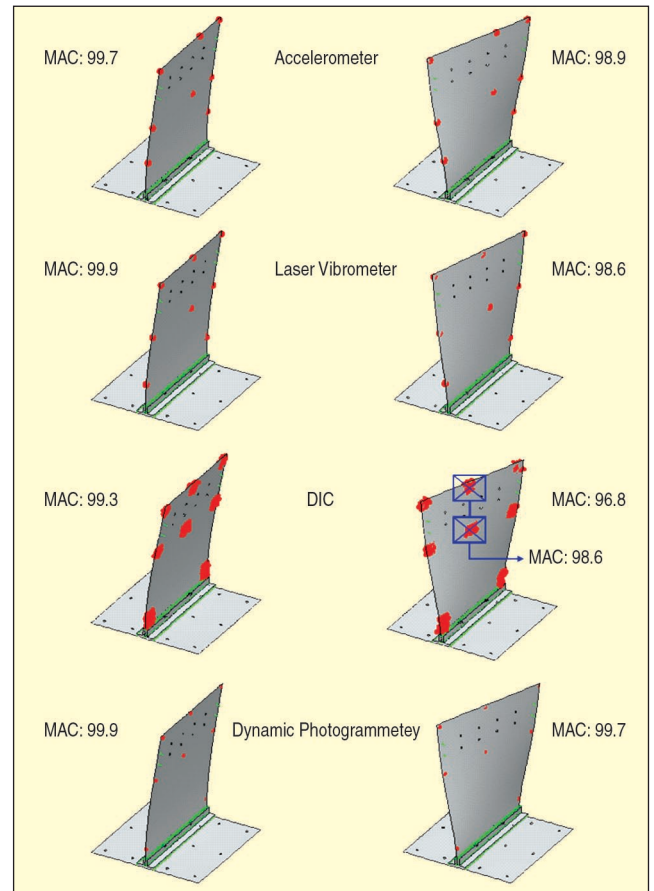


Figure 11. FEM to test correlation results for the various methods, for modes 1 (26 Hz) and 3 (71 Hz).

Correlation of BU Structure Modal Data. To evaluate the performance of the four measurement techniques, MAC values were calculated using the FEMtools software package.²¹ Overlay plots of the four experimental approaches and the finite-element model can be seen in Figure 11. Tables 2 and 3 summarize the correlation results for Modes 1 and 3, respectively, comparing all methods.

Overall, the results are very good. The accelerometer and laser MAC values were all above 99.5 when compared to the FEM for the two modes evaluated. When dynamic photogrammetry (DP) was used, MACs of at least 99.7 were obtained. DIC yielded the slightly lower results for both Modes 1 and 3, with values of 99.3 and 97.8, respectively. Originally, the value between the FEM and the DIC measurement for Mode 3 was 96.8, but removing the center two patches improved the MAC by a full point. These patches lie along what is essentially the node line for the torsion mode of the upright. The structure exhibits little to no response in this area, so the measurement will have the lowest signal-to-noise ratio.

Table 2. Comparison of MAC values for Mode 1.

Case	Laser Mode 1	Accel. Mode 1	DIC Mode 1	DP Mode 1	FE Model
Laser Mode 1	100	99.5	99.7	99.8	99.9+
Accel. Mode 1	99.5	100	99.7	99.6	99.8
DIC Mode 1	99.7	99.7	100	99.4	99.3
DP Mode 1	99.8	99.6	99.4	100	99.9

Table 3. Comparison of MAC values for Mode 3.

Case	Laser Mode 3	Accel. Mode 3	DIC Mode 3	DP Mode 3	FE Model
Laser Mode 3	100	98.4	99.6	99.5	99.6
Accel. Mode 3	98.4	100	97.3	98.5	99.5
DIC Mode 3	99.6	97.3	100	95.6	97.8
DP Mode 3	99.5	98.5	95.6	100	99.7

Removing the points reduced the variance between the measurement and the model.

When comparing two experimental sets, the purity of the finite-element model's mode shapes is lost, and variance on the measurements can compound to provide biased results. In this case, however, good correlation was obtained for both Modes 1 and 3; all MAC values were 95.6 and higher when the empirical results from two different approaches were correlated.

Observations and Interpretation of Results

Each technique applied in this comparison has its advantages and drawbacks, but in the end, all yielded good, consistent measurements. The biggest difference between traditional and optical techniques is the approach taken to measure multiple modes. Accelerometers and laser vibrometers measure multiple modes over a broad frequency range point by point. Conversely, the two optical approaches measure all points simultaneously, one mode at a time.

Accelerometers provide an inertial reference frame, so establishing the calibration and orientation procedures (required by the scanning laser vibrometer and optical measurements) can be simpler. However, mass loading has to be taken into consideration, especially when performing a test that requires numerous or roving accelerometers.

The laser Doppler vibrometer has the widest dynamic capabilities, since it can measure velocities from as low as a few Hz up to 80 kHz. Low-frequency measurements must be taken with care. When the laser is stationary, not tracking the global motion of the test article, the effective measurement point is constantly moving on the structure when high displacements or large rigid-body movements are present.

The main advantages of digital image correlation are the immense number of effective measurement points and the fact that strain throughout these patches can be measured directly. With the analysis configuration chosen (facet settings), each patch – about 3 × 3 inches – had on average of 400 effective measurement points. Had the entire face been patterned while maintaining the same resolution, the number of points measured would have been on the order of 30,000 to 40,000 points. Note that the laser vibrometer has the ability to sequentially measure a comparable number of points, but the time needed to acquire the data would be quite large – on the order of 10 hours or more. In either case, the limiting factors become processing power and memory.

As opposed to tracking facets of pixels from image to image, dynamic photogrammetry tracks the 3D motion of circular targets. The number of measurement points is on the order of the more traditional modal tests, so the computation time relative to DIC is greatly reduced. Because discrete targets are spatially well separated, local strain cannot be readily calculated as with DIC. A benefit to either optical technique is their ability to measure high amounts of rigid-body motion. Cabling and tracking of the targets do not have to be considered as long as the test piece remains within the field of view. Conversely, the primary disadvantage to both optical approaches is that the low-amplitude displacements associated with high-frequency vibrations can fall below the noise floor of the optical measurement. When mode shapes are to be measured, these optical tests require at least a partial modal test in preparation of FNM testing as well as feedback transducers (accelerometers or vibrometers).


Conclusions

The results of this study show that digital image correlation and dynamic photogrammetry can be used to measure mode shapes that correlate very well to those obtained using accelerometers and laser Doppler vibrometers. All four measurement approaches were used to acquire the lower-order modes of the structures studied and then were correlated to each other as well as a highly accurate finite-element model. Excellent correlation of the measurement results was obtained using each of the different measurement approaches. Strengths, limitations and comparison of the different approaches were discussed.

Acknowledgement

Some of the work presented herein was partially funded by the U.S. Army Research Office (Nanomanufacturing of Multifunctional Sensors Grant) and also by the U.S. Army Aviation and Missile Command, Redstone Arsenal. The authors would also like to thank Tim Schmidt of Trillion Quality Systems for providing insight and providing necessary equipment to conduct some of the measurements presented in this paper. The authors are grateful for the support obtained.

References

1. Warren, C., Niezrecki, C., and Avitabile, P., "Applications of Digital Image Correlation and Dynamic Photogrammetry for Rotating and Nonrotating Structures," Proceedings of the 7th International Workshop on Structural Health Monitoring, Stanford, CA, September 2009.
2. Helfrick, M., Niezrecki, C., and Avitabile, P., "3D Digital Image Correlation Methods for Full-Field Vibration Measurement," Proceedings of the Twenty Sixth International Modal Analysis Conference, Orlando, FL, February 2008.
3. Helfrick, M., Niezrecki, C., and Avitabile, P., "Optical Noncontacting Vibration Measurement of Rotating Turbine Blades," Proceedings of the Twenty Seventh International Modal Analysis Conference, Orlando, FL, February 2009.
4. Wu, P., Stanford, B., Bowman, W., and Ifju, P., "Digital Image Correlation Techniques for Full-Field Displacement Measurements of Micro Air Vehicle Flapping Wings," *Experimental Techniques*, pp. 53-58, November/December 2010.
5. Paulsen, U. S., Erne, O., Moeller, T., Sanow, G., Schmidt, T., "Wind Turbine Operational and Emergency Stop Measurements Using Point Tracking Videogrammetry," Proceedings of the 2009 SEM Annual Conference and Exposition, Albuquerque, NM, June 4, 2009.
6. Mikhail, E., Bethel, J., and McGlone, J., *Introduction to Modern Photogrammetry*, John Wiley and Sons, 2001.
7. Lecompte, D., Smits, A., Bossuyt, S., Sol, H., Vantomme, J., Van Hemelrijck, D., and Habraken, A. M., "Quality Assessment of Speckle Patterns for Digital Image Correlation," *Optics and Lasers in Engineering*, Vol. 44, No 11, pp. 1132-1145, November 2006.
8. Peters, W. H., Ranson, W. F., Sutton, M. A., Chu, T. C., Anderson, J., "Application of Digital Image Correlation Methods to Rigid Body Mechanics," *Opt. Eng.*, Vol. 22, No. 6, pp. 738-42, 1983.
9. Chu, T. C., Ranson, W. F., and Sutton, M. A., "Applications of Digital-Image Correlation Techniques to Experimental Mechanics," *Experimental Mechanics*, Vol. 25, No. 3, pp. 232-244, 1985.
10. Kahn-Jetter, Z. L., and Chu, T. C., "Three-Dimensional Displacement Measurements Using Digital Image Correlation and Photogrammetric Analysis," *Experimental Mechanics*, Vol. 30, No. 1, pp. 10-16, 1990.
11. Luo, P. F., Chao, Y. J., Sutton M. A., and Peters, W. H., "Accurate Measurement of Three-Dimensional Deformations in Deformable and Rigid Bodies Using Computer Vision," *Experimental Mechanics*, Vol. 33, No. 2, June 1993.
12. Sutton, M. A., Orteu, J. J., Schreier, H., *Image Correlation for Shape, Motion and Deformation Measurements: Basic Concepts, Theory and Applications*, Springer Science+Business Media, LLC, ISBN#: 978-0-387-78746-6, 2009.
13. Schmidt, T. Tyson, J. and Galanulis, K., "Full-Field Dynamic Displacement and Strain Measurement Using Advanced 3D Image Correlation Photogrammetry: Part I," *Experimental Techniques*, Vol. 27, No. 3, pp. 47-50, 2003.
14. Schmidt, T. Tyson, J. and Galanulis, K., "Full-Field Dynamic Displacement and Strain Measurement Using Advanced 3D Image Correlation Photogrammetry: Part II", *Experimental Techniques*, Vol. 27, No. 4, pp. 22-26, 2003.
15. ARAMIS, v. 5.3.0 User's Manual, Revision A, GOM mbH, Braunschweig, Germany, 2004.
16. Butland, A., "A Reduced Order, Test Verified Component Mode Synthesis Approach for System Modeling Applications," Master of Science Thesis, University of Massachusetts Lowell, January 2008.
17. Nicgorski, D. "Investigation on Experimental Issues Related to Frequency Response Function Measurements for Frequency Based Substructuring," Master of Science Thesis, University of Massachusetts Lowell, January 2008.
18. Wirkkala, N.A., "Development of Impedance Based Reduced Order Models for Multi-Body Dynamic Simulations of Helicopter Wing Missile Configurations," Master of Science Thesis, University of Massachusetts Lowell, April 2007.
19. Pingle, P., Sailhamer, J., and Avitabile, P., "Comparison of 3D Laser Vibrometer and Accelerometer Frequency Measurements," Proceedings of the IMAC-XXVII, Orlando, FL, February 9-12, 2009.
20. LMS Test.Lab – Leuven Measurement Systems, Leuven, Belgium.
21. FEMtools 3.0 – Dynamic Design Solutions, Leuven, Belgium Polytec Scanning Laser Doppler Vibrometer, Polytec Optical Measurement Systems.
22. PONTOS v6.2 User Manual - Mittelweg 7-8, D-38106 Braunschweig, Germany, 2009. 

The author can be reached at: Peter_Avitabile@uml.edu.